

# Embedding networks with the random walk first return time distribution

Vedanta Thapar\*, Renaud Lambiotte\*, and George T. Cantwell†

**Abstract.** We propose the first return time distribution (FRTD) of a random walk as an interpretable and mathematically grounded node embedding. The FRTD assigns a probability mass function to each node, allowing us to define a distance between any pair of nodes using standard metrics for discrete distributions. We present several arguments to motivate the FRTD embedding. First, we show that FRTDs are strictly more informative than eigenvalue spectra, yet insufficient for complete graph identification, thus placing FRTD equivalence between cospectrality and isomorphism. Second, we argue that FRTD equivalence between nodes captures structural similarity. Third, we empirically demonstrate that the FRTD embedding outperforms manually designed graph metrics in network alignment tasks. Finally, we show that random networks that approximately match the FRTD of a desired target also preserve other salient features. Together these results demonstrate the FRTD as a simple and mathematically principled embedding for complex networks.

**1. Introduction.** Network science attempts to provide the tools to understand the structure and function of high-dimensional interconnected systems [27, 28, 25]. The most basic form of network analysis is descriptive—understanding networks or nodes with simple summary statistics. A problem of particular interest is *network embedding*, namely, representing nodes as vectors in an appropriate space so that structural properties of the network are encapsulated [15]. Network embeddings play a crucial role in a wide range of data science tasks including community detection and node classification [36, 20, 7].

There are many methods for embedding networks. One strategy is to represent each node using a handful of heuristic metrics such as degree, clustering coefficient, or centrality measures [9]. More advanced machine learning methods capture richer global patterns; many rely on spectral information derived from the graph Laplacian or the properties of random walk processes [32, 18, 33, 21]. However, machine-learning embedding methods are not without issue. First, learning-based approaches may be stochastic and hence do not necessarily identify automorphically equivalent nodes with the same embedding, even though they are indistinguishable from a structural perspective. Second, they may suffer from poor interpretability due to opaque neural network based transformations of graph features.

In this work we propose the first return time distribution (FRTD) of a random walk as an embedding for network nodes. We focus on undirected networks but the approach is easily extended to weighted and directed networks. We find that the FRTD captures meaningful structural information in a simple representation, mapping each node to a one-dimensional discrete probability distribution.

Several motivations underlie this study of random walk return embeddings. Prior work has shown that random walk-based embeddings can enhance the performance of graph neural networks [48, 12] and that diffusion kernels yield effective graph embeddings [10, 37]. Additionally, random walk returns are invariant under node relabeling and, although not

\*The Mathematical Institute, University of Oxford, Oxford OX2 6GG, United Kingdom ([vedanta.thapar@maths.ox.ac.uk](mailto:vedanta.thapar@maths.ox.ac.uk), [renaud.lambiotte@maths.ox.ac.uk](mailto:renaud.lambiotte@maths.ox.ac.uk)).

†Department of Engineering, University of Cambridge, Cambridge CB2 1PZ, United Kingdom ([gtc31@cam.ac.uk](mailto:gtc31@cam.ac.uk)).

invertible (that is, the FRTD does not uniquely determine the graph), we believe the corresponding preimage is typically very small and almost always unique. We further demonstrate that FRTD information is strictly richer than the eigenspectrum alone, situating it between graph cospectrality and full isomorphism.

In contrast to prior work, we advocate specifically for the *first* return time distribution, which to our knowledge is not currently used. The shift is important because the FRTD is a distribution and hence normalized to sum to unity. On the other hand, return time probabilities (i.e., not the *first* returns) converge to a constant that depends only on node degree. The consequence is that the distance between (non-first) return time probabilities is only finite for nodes of the same degree.

We define notions for FRTD-equivalence and FRTD-distance between both nodes and graphs. To illustrate the practical utility of the FRTD as an embedding, we present three applications: role extraction, alignment, and randomization.

First, we consider the problem of grouping nodes into roles. In a graph, nodes are considered to have similar roles if they are somehow structurally similar to each other [6, 8]. We see that the FRTD embedding places nodes close together if they play a similar structural role in a network. In contrast, embeddings based on diffusion-type dynamics are designed such that proximity in the embedding corresponds to proximity in the network [36]; clustering nodes according to their first return time distributions yields partitions distinct from traditional community structure.

Second, we experimentally assess graph alignment algorithms that leverage FRTDs: nodes in two networks are identified with each other so as to minimize the FRTD distances. We show that the FRTD can be used to inform and improve existing alignment algorithms such as FUGAL [5], which otherwise rely on heuristic network embeddings.

Finally, we look at how FRTDs can be used to randomize a network so that structural features are approximately preserved. The configuration model, for example, provides a simple method for randomizing a graph while preserving the degree sequence. However, it fails to preserve the vast majority of interesting features such as triad counts, spectral features, or centrality rankings [27]. The upshot is that this method does not create realistic looking networks. It is an open problem to find a general purpose model that can generate networks that look realistic. We show how the FRTD embedding can be used to define a model that interpolates between the  $G(n, m)$  random graph ensemble and a model that preserves significant higher-order structure.

Taken together our arguments provide converging lines of evidence that the FRTD is a principled and useful method for embedding networks.

## 2. Theory.

**2.1. Notation and background.** We consider undirected (but possibly weighted) graphs,  $G = (V, E)$  ( $|V| = n$ ,  $|E| = m$ ). Without loss of generality, we assume  $V = \{1, 2, \dots, n\}$ , and hence the graph is defined by an  $n \times n$  symmetric adjacency (or weight) matrix

$$(2.1) \quad A_{ij} = \begin{cases} w_{ij} & \text{if } (i, j) \in E \\ 0 & \text{otherwise} \end{cases},$$

where  $w_{ij} = 1$  for an unweighted network. We will additionally assume weights to be positive, i.e.,  $w_{ij} > 0$ . The degree of node  $i$  is the sum over its edges,  $d_i = \sum_j A_{ij}$ , and the diagonal degree matrix has elements

$$(2.2) \quad D_{ii} = d_i = \sum_j A_{ij}.$$

A random walk  $(u_0, u_1, \dots)$  that is currently at node  $i$  will move to neighbor  $j$  with probability

$$(2.3) \quad P[u_{t+1} = j | u_t = i] = \frac{A_{ij}}{d_i},$$

or in matrix notation the transition matrix is  $\mathbf{D}^{-1}\mathbf{A}$ . To study the behavior of random walks we will pay particular attention to the symmetric normalized adjacency matrix

$$(2.4) \quad \mathbf{X} = \mathbf{D}^{-1/2}\mathbf{A}\mathbf{D}^{-1/2} = \mathbf{D}^{1/2}(\mathbf{D}^{-1}\mathbf{A})\mathbf{D}^{-1/2}.$$

Note that  $\mathbf{X}$  is real and symmetric and hence has real eigenvalues. Further, because  $\mathbf{D}^{-1}\mathbf{A}$  is a stochastic matrix, and because  $\mathbf{X}$  is related to this through a similarity transformation, the eigenvalues of  $\mathbf{X}$  are in  $[-1, 1]$ .

**2.2. First return time distributions.** Denote by  $f_i(t)$  the probability that a random walk that starts at node  $i$  will return to  $i$  for the first time after exactly  $t$  steps,

$$(2.5) \quad f_i(t) = P[u_t = i, u_s \neq i \text{ for } 0 < s < t | u_0 = i].$$

This is the *first return time distribution* (FRTD) for node  $i$ . Our proposal is to interpret  $f_i(t)$  as an embedding for node  $i$ , i.e., to associate node  $i$  with the vector  $\mathbf{f}_i$ . We immediately see the embedding is normalized since, on any finite network, a random walk must eventually return and so  $\sum_t f_i(t) = 1$ . From the FRTD we define the following notions of equivalence.

**Definition 2.1 (FRTD equivalent nodes).** Let  $f_i^{(G_1)}(t)$  be the FRTD of node  $i$  in network  $G_1$ , and  $f_j^{(G_2)}(t)$  be the FRTD of node  $j$  in network  $G_2$ . We say these nodes are FRTD-equivalent if  $f_i^{(G_1)}(t) = f_j^{(G_2)}(t)$  for all  $t$ .

**Definition 2.2 (FRTD equivalent graphs).** Two graphs  $G_1 = (V_1, E_1)$  and  $G_2 = (V_2, E_2)$  are FRTD equivalent if there is a bijection between the nodes  $\pi : V_1 \rightarrow V_2$  such that each  $i \in V_1$  is FRTD equivalent to  $\pi(i) \in V_2$ .

Note that automorphically equivalent nodes (those in the same orbit) must be FRTD equivalent. However, the converse is not true, as shown in the counter-example of Fig. 1(a).

To further analyze FRTDs, it is convenient to work with their generating functions. The first return times at node  $i$  are generated by

$$(2.6) \quad F_i(z) = \sum_{t=0}^{\infty} z^t f_i(t),$$

which has the following useful representation.

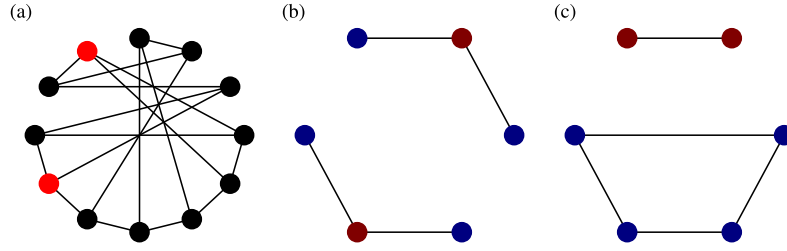


Figure 1: In panel (a) we show the Frucht graph [16]. The two red nodes are not automorphically equivalent but share the same first return time distributions. In (b) and (c) we give the smallest example of two non-isomorphic graphs that are FRTD equivalent, the nodes are colored according to FRTD equivalence across the two graphs.

**Lemma 2.3.** *For an undirected graph with normalized adjacency matrix  $\mathbf{X}$ , let  $\{\lambda_\alpha\}_{\alpha=1}^N$  be the  $N$  distinct eigenvalues of  $\mathbf{X}$  with multiplicities  $\{N_\alpha\}_{\alpha=1}^N$  and corresponding orthonormal eigenvectors  $\{\psi_{\alpha\beta}\}_{\beta=1}^{N_\alpha}$ . Then,*

$$(2.7) \quad F_i(z) = 1 + \left( \sum_{\alpha=1}^N \frac{\sum_{\beta=1}^{N_\alpha} (\psi_{\alpha\beta i})^2}{\lambda_\alpha z - 1} \right)^{-1}.$$

*Proof.* First return times at node  $i$  are generated by  $F_i(z)$  and  $k$ th return times are generated by  $F_i(z)^k$ . Returns of any order are thus generated by  $\sum_{k=0}^{\infty} F_i(z)^k = (1 - F_i(z))^{-1}$ . At the same time, the probability of a return of any order at time  $t$  is  $(\mathbf{D}^{-1}\mathbf{A})_{ii}^t = (\mathbf{X}^t)_{ii}$  and hence

$$(2.8) \quad (1 - F_i(z))^{-1} = \sum_{t=0}^{\infty} z^t (\mathbf{X}^t)_{ii} = \sum_{t=0}^{\infty} z^t \sum_{\alpha=1}^N \lambda_\alpha^t \sum_{\beta=1}^{N_\alpha} (\psi_{\alpha\beta i})^2 = \sum_{\alpha=1}^N \frac{\sum_{\beta=1}^{N_\alpha} (\psi_{\alpha\beta i})^2}{1 - \lambda_\alpha z},$$

from which Eq. (2.7) immediately follows. ■

With this representation for the generating function  $F_i(z)$  we quickly find the following results.

**Theorem 2.4.** *We denote the eigenvalues and eigenvectors of the symmetric normalized adjacency matrix of  $G_1$  by  $\lambda_\alpha^{(G_1)}$  and  $\{\psi_{\alpha\beta}^{(G_1)}\}_{\beta=1}^{N_\alpha^{(G_1)}}$ , and likewise for  $G_2$ . Then, node  $i \in G_1$  and  $j \in G_2$  are FRTD-equivalent if and only if*

- (i)  $\lambda_\alpha^{(G_1)} = \lambda_\alpha^{(G_2)}$  (random-walk cospectrality) and
- (ii)  $\sum_{\beta=1}^{N_\alpha^{(G_1)}} (\psi_{\alpha\beta i}^{(G_1)})^2 = \sum_{\beta=1}^{N_\alpha^{(G_2)}} (\psi_{\alpha\beta j}^{(G_2)})^2$

for all  $\alpha$ .

*Proof.* One direction is immediate: If the eigenspectra conditions of (i) and (ii) are met then by the spectral representation of Lemma 2.3 the generating functions  $F_i^{(G_1)}(z) = F_j^{(G_2)}(z)$  and so the distributions are identical.

Conversely, if  $f_i^{(G_1)}(t) = f_j^{(G_2)}(t)$  for all  $t$  then  $F_i^{(G_1)}(z) = F_j^{(G_2)}(z)$ . Additionally, note that the function  $(F_i^{(G_1)}(z) - 1)^{-1}$  has simple poles at  $1/\lambda_\alpha^{(G_1)}$  and these poles have residue  $\sum_{\beta=1}^{N_\alpha^{(G_1)}} (\psi_{\alpha\beta i}^{(G_1)})^2 / \lambda_\alpha^{(G_1)}$ . The equivalent statement for  $(F_j^{(G_2)}(z) - 1)^{-1}$ , together with the requirement of equality of poles and residues, establishes the theorem.  $\blacksquare$

If we compare two nodes in the same graph then the matching eigenvalues in condition (i) of Theorem 2.4 is trivial. Hence,

**Corollary 2.5.** *Two nodes  $i$  and  $j$  in the same graph are FRTD-equivalent if and only if  $\sum_{\beta=1}^{N_\alpha} (\psi_{\alpha\beta i})^2 = \sum_{\beta=1}^{N_\alpha} (\psi_{\alpha\beta j})^2$  for all  $\alpha$ .*

Theorem 2.4 requires that FRTD-equivalent graphs have the same eigenvalues for their normalized adjacency matrix. We call such graphs *cospectral*. However, FRTD-equivalence is strictly stronger than cospectrality. To see this, note that the 4-cycle  $C_4$  and the 3-star  $S_3$  both have eigenvalues  $(-1, 0, 0, 1)$  but are clearly not FRTD-equivalent.

At the same time, FRTD-equivalence is weaker than isomorphism as the counter-example in Fig. 1 shows. Hence, FRTD-equivalence sits between isomorphism and cospectrality. Although it has not been proved, non-isomorphic cospectral graphs in the (non-normalized) adjacency matrix appear to be exceedingly rare [19, 44]. For this reason we conjecture that almost all graphs have no FRTD-equivalent twins that are not isomorphic.

**2.3. Node and graph distances.** While exact FRTD equivalence may be rare, our central contention is that if two nodes (resp. graphs) have similar but not identical FRTDs, those nodes (resp. graphs) are meaningfully similar to one another. To complete the interpretation of  $f_i(t)$  as an embedding we must additionally choose a distance metric,  $d(\mathbf{f}_i, \mathbf{f}_j)$ . Any distance between probability mass functions is a possible candidate for  $d$ , though in this work we consider the total variation distance

$$(2.9) \quad d(\mathbf{f}_i, \mathbf{f}_j) = \frac{1}{2} \sum_{t=0}^{\infty} |f_i(t) - f_j(t)|.$$

The total variation is a bounded distance metric between distributions with a maximum value of 1. Note, however, it does not define a metric between nodes since  $d(\mathbf{f}_i, \mathbf{f}_j) = 0$  does not imply  $i = j$ .

The node-level measure can be aggregated to define a distance between graphs,

$$(2.10) \quad d(G_1, G_2) = \frac{1}{2n} \sum_{i=1}^n d(\mathbf{f}_i^{(G_1)}, \mathbf{f}_i^{(G_2)})$$

and note that if  $d(G_1, G_2) = 0$  then  $G_1$  and  $G_2$  are FRTD-equivalent.

Again, while exact FRTD equality may be exceedingly rare we contend that small values for  $d(\mathbf{f}_i, \mathbf{f}_j)$  or  $d(G_1, G_2)$  imply that the nodes or graphs are meaningfully similar, and for this reason  $\mathbf{f}_i$  is a sensible embedding of the nodes. In the remaining sections of this paper we present a sequence of experiments to provide evidence for our claim that FRTD embeddings encode meaningful properties of graphs.

**3. Empirical study of FRTDs.** If the FRTD is a good embedding then it should be useful for downstream tasks. We now present experiments using the FRTD for role extraction, graph alignment, and graph randomization.

**3.1. Role extraction.** Identifying meaningful groupings of nodes is a standard task for summarizing and analyzing networks. Much of this work focuses on community structure [14], and often assortative community structure where nodes are assumed to connect preferentially to nodes in their same group. However, we believe that the FRTD similarity does not speak to this issue. For example, in the stochastic block model—the main generative model for community structure—nodes that are in different groups may well have the same FRTD [22].

We propose that the FRTD does not distinguish nodes based on community structure but rather roles. Intuitively, two nodes have the same role if they are structurally similar, regardless of their mutual proximity or community membership [35]. There are a variety of approaches to role extraction such as generalized block-modeling [11] or clustering of node self-similarity measures [8, 6]. The machine learning literature has also addressed the problem, for example RolX [21] which uses node features (such as degree, triangle count, etc.) to cluster roles. A review of approaches can be found in [36].

To assign structural roles to nodes we apply spectral clustering to the FRTD. Spectral clustering is a standard off-the-shelf method to cluster points with a notion of pair-wise distance [43]. It proceeds by applying  $k$ -means clustering to the leading eigenvectors of the matrix  $s_{ij} = e^{-d(f_i, f_j)}$ . In all clustering analyses, we use the default options in the scikit-learn library [31].

In Fig. 2 we study a simple example with easily interpretable clusters. We compare FRTD based embeddings to other classic embedding methods.

In Fig. 3 we look at three network data sets. Specifically, we look at networks of (i) flights between airports, (ii) character co-occurrences in the Lord of the Rings books and, (iii) connections between neurons in *C. elegans*.

**3.1.1. Air transit network.** The world air transit network from the OpenFlights dataset 2016<sup>1</sup> is a network in which nodes represent airports and edges indicate the existence of at least one direct flight between them. The number and directionality of flights have been ignored, yielding an unweighted, undirected network. Airport sizes were taken from the OurAirports dataset<sup>2</sup>.

We cluster the nodes into three groups by applying spectral clustering to the FRTD. For the flight network, we find clusters that roughly correspond to small, medium, and large airports (see Table 1). Importantly, this structure is not identified by standard network clustering. In addition to the FRTD clusters, in Fig. 3 we show the results of spectral clustering applied to the adjacency matrix and the Louvain algorithm [4]. While clustering the FRTD picks out airport classes, traditional clustering largely picks out geography.

**3.1.2. Lord of the Rings character network.** For the Lord of the Rings example, an undirected but weighted network was constructed in which each node is a character and an

<sup>1</sup>Upstream: [openflights.org](http://openflights.org), retrieved from [networks.skewed.de/net/openflights](http://networks.skewed.de/net/openflights)

<sup>2</sup>[ourairports.com/data](http://ourairports.com/data)

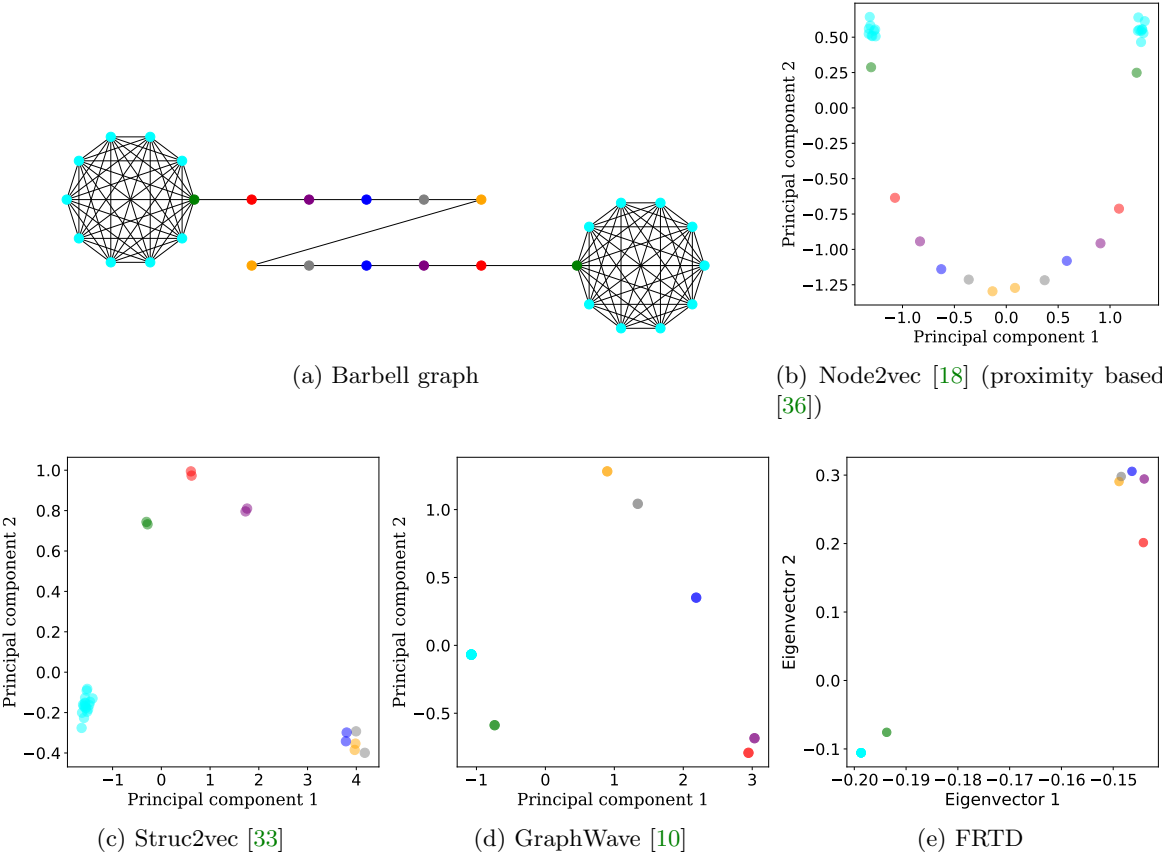


Figure 2: Principal component visualization of different embedding methods for the Barbell graph. Embeddings are calculated with the default parameters for all the algorithms. Node2vec is a proximity based embedding method and places nodes that are close to each other in the graph close in the embedding space. The other methods are structural (role) based [36]. Notably struc2vec does not tend to identify automorphically equivalent nodes with the same embeddings. In contrast, GraphWave assigns structurally equivalent nodes to arbitrarily close embeddings (with appropriate hyper-parameter selection) and FRTD embeddings are always exactly equivalent for automorphic nodes.

edge is introduced between two characters if they co-occur in the same chapter<sup>3</sup>. Edges are weighted by the number of such co-occurrences.

We again cluster the nodes into three groups by applying spectral clustering to the FRTD, and the results are in Fig. 3. The three groups correspond to main (e.g., Frodo, Gandalf, and Sauron), supporting, and peripheral characters (see Table 2 for full details). Again, this structure is not identified by traditional community detection. This is due to the narrative

<sup>3</sup>See [lotrproject.com/statistics/books/cooccurrences](http://lotrproject.com/statistics/books/cooccurrences)

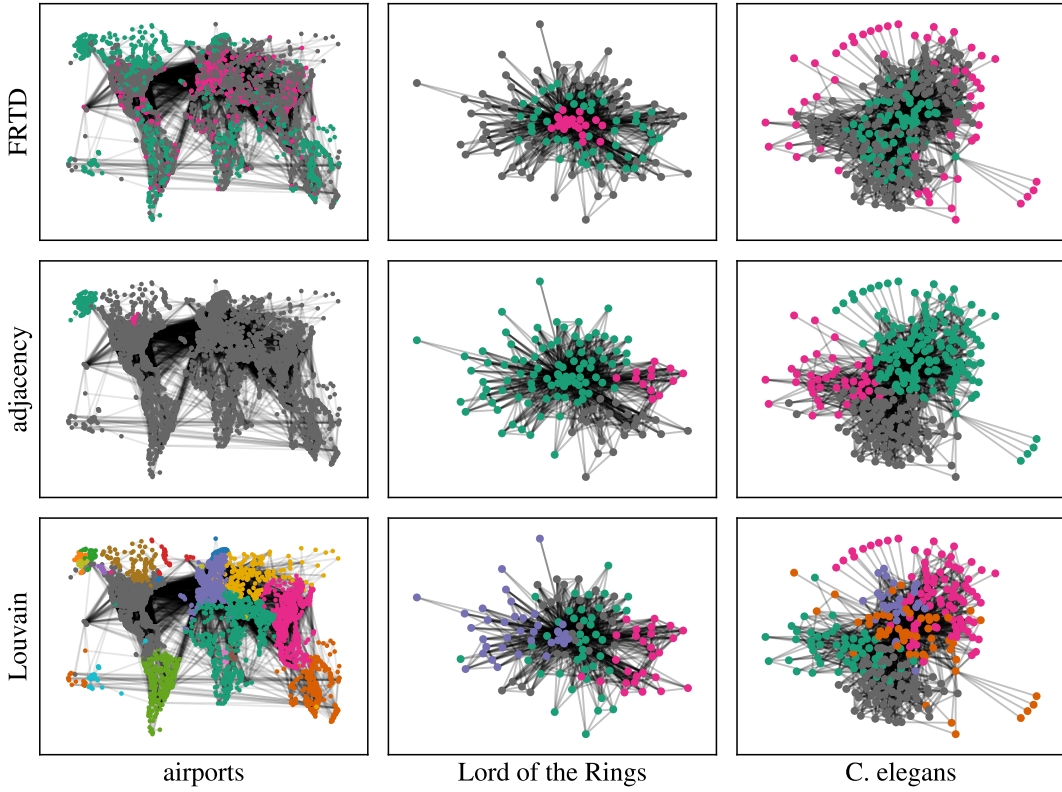


Figure 3: Clustering three example networks, namely the airports, Lord of the Rings, and *C. elegans* networks, described in Sec. 3.1. We show clusters found from the FRTD, adjacency matrix, and the Louvain algorithm. Nodes in the airports network are placed by latitude and longitude, the other two networks are drawn using the Fruchterman-Reingold force-directed algorithm [17]. While the FRTD clusters pick out structural roles—nodes with similar structural positions in the network—the adjacency and Louvain clusters pick out nodes that are proximate in the network.

structure of the books—much of the plot unfolds in parallel distant storylines and thus many key characters rarely appear together yet remain central to the plot. This highlights the use of FRTD-based role extraction in revealing functional roles that may not be defined by proximity. The FRTD clusters are hence complementary and largely orthogonal to classic community structure.

**3.1.3. *C. elegans* neural network.** The connectome of the *C. elegans* worm was the first fully mapped brain network of neurons and their synaptic connections [46]. The network we use has 297 nodes and while the original data is directed we consider the undirected and unweighted version. Comparison of the three clustering algorithms tells a similar story. The FRTD picks out nodes that are structurally similar but not proximate, for example, leaf nodes

are placed in the same cluster. In contrast, the other methods find groups of nodes that are more well connected to each other than might be expected by chance.

In summary, two nodes that are similar in FRTD will play similar structural roles in the network, regardless of the other properties of nodes or the other that they connect to.

**3.2. Alignment.** We now turn to graph alignment. Two graphs  $G_1$  and  $G_2$  are assumed to be on the same set of nodes. However, the identification of nodes in  $G_1$  with those in  $G_2$  is unknown and the task of graph alignment is to find this mapping. Usually we seek a mapping between the nodes so that the (labeled) topology is very close between the two graphs. We refer to Ref. [41] for a review.

To make this task a well-posed mathematical problem, we ask for a permutation  $\pi$  such that the following (squared) Frobenius norm is minimized

$$(3.1) \quad L(\pi) = \|\mathbf{A}^{(1)}\pi - \pi\mathbf{A}^{(2)}\|_F^2,$$

where  $\mathbf{A}^{(1)}$  is the adjacency matrix of  $G_1$ , and likewise for  $G_2$ . That is to say, we seek  $\pi = \arg \min_{\pi'} L(\pi')$ . Clearly the  $\min_{\pi'} L(\pi') = 0$  if and only if the graphs are isomorphic. However, the optimization is well defined even when no zero solution exists, and hence alignment can be considered a relaxation of the isomorphism problem [1].

Minimizing Eq. (3.1) is a quadratic assignment problem and is hence NP-hard. In general, efficient algorithms will not find the global minimum but many fast heuristics have been developed, such as gradient descent methods (see Ref. [42]). One approach maps the problem to a linear sum assignment by defining a cost matrix  $C_{ij}$  which assigns a cost to matching a node in  $i \in G_1$  to  $j \in G_2$ , i.e., we instead look for the bijection  $\pi : V_1 \rightarrow V_2$  that minimizes

$$(3.2) \quad \sum_i C_{i,\pi(i)},$$

and the minimum can be found with  $\mathcal{O}(n^3)$  operations by, e.g., the Hungarian algorithm [24]. This cost  $C_{ij}$  is typically assigned by defining a notion of distance between nodes.

The linear assignment of Eq. (3.2) will not generally be equivalent to the full quadratic problem of Eq. (3.1). The quality of the solution will depend on how well the structure is captured by the entries of  $\mathbf{C}$ . The most competitive approaches combine both and minimize

$$(3.3) \quad \|\mathbf{A}^{(1)}\pi - \pi\mathbf{A}^{(2)}\|_F^2 + \mu \operatorname{Tr}(\pi^T \mathbf{C}),$$

which allows the matrix  $\mathbf{C}$  to guide the heuristic solver for the quadratic assignment problem. This is the approach of Feature-Fortified Unrestricted Graph Alignment (FUGAL) [5], which defines  $\mathbf{C}$  by a grab-bag of node features such as, such as degrees, neighbor degrees, and clustering coefficients.

Instead of reaching for a battery of hand selected features, we believe the FRTD captures many of the relevant structural properties. For this reason we propose setting  $C_{ij} = d(\mathbf{f}_i^{(G_1)}, \mathbf{f}_j^{(G_2)})$ . We insert this cost matrix directly into the FUGAL algorithm's approximate solver and henceforth refer to this as FUGAL-FRT.

To experimentally assess the method, we produce corrupted copies of graphs and attempt to recover the alignment. We follow Ref. [38] and consider benchmarking examples as follows:

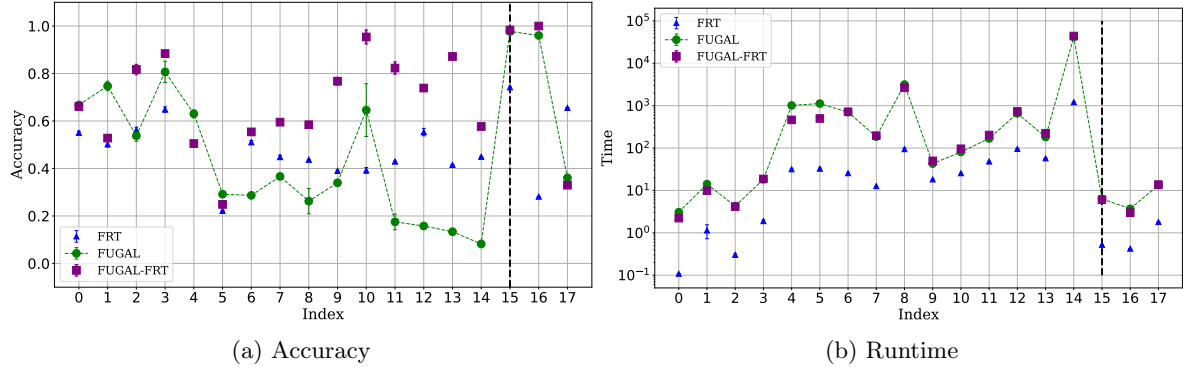


Figure 4: Performance of three alignment algorithms on a set of 18 undirected network datasets ordered by number of edges—see Appendix C for details. For the first 15 graphs, the noisy copy is created by randomly removing 5% of edges and permuting the nodes. For the last three networks, ‘real’ noise is used (see Appendix C for details). All experiments were run with the same hyperparameters ( $\mu = 1$ ) and no optimization of hyperparameters was considered.

- Input graph  $G_1$  and initialize graph  $G_2$  by copying  $G_1$ .
- Randomly remove  $x\%$  of edges in  $G_2$ .
- Permute the node labels in  $G_2$ , with this permutation serving as the “ground truth” mapping.

We can repeat the process several times to produce a set of pairs of graphs  $(G_1, G_2)$  with known alignments. To measure the quality of a recovered permutations  $\pi$  we compute the proportion of correctly aligned nodes.

We compare three different methods, namely FUGAL, FUGAL-FRT, and a pure linear assignment using only the FRTDs. We test the approach on the networks previously used in Ref. [38]. Figure 4 shows the performance of the methods, we see that FRTD linear alignment is often less accurate than FUGAL and FUGAL-FRT, but it runs significantly faster in all cases.

More importantly, FUGAL-FRT generally performs better than the classic FUGAL, often considerably so. This is notable because while FUGAL uses a variety of intuitively motivated metrics to embed nodes, FUGAL-FRT only use the FRTD. This provides further evidence the the FRTD contains a rich variety of structural information about nodes, and that being close in FRTD is a strong indication that nodes are structurally similar.

**3.3. Network randomization.** Through the experiments of the previous two sections we have started to provide evidence that FRTDs are a meaningful embedding for nodes. We now turn to the question of how well the FRTDs capture the whole structure of a network. To this end, we consider whether the FRTDs form a suitable basis for network randomization.

We consider a random graph ensemble that interpolates between the Erdős–Rényi random graph  $G(n, m)$ , i.e., uniform over all graphs on  $n$  nodes with  $m$  edges, and a model that preserves the full FRTD. Given a graph  $G$ , we generate a randomized version of it with the

same number of edges. Graph  $G'$  is sampled with probability

$$(3.4) \quad P_G(G') = \frac{e^{-\beta d(G, G')}}{Z_{G, \beta}},$$

where the parameter  $\beta$  is an inverse temperature,  $d$  is the FRTD distance between the graph  $G'$  and the target graph  $G$ , and  $Z_{G, \beta}$  is a normalizing constant that does not depend on  $G'$ . We sample from the distribution with Markov chain Monte Carlo (MCMC) and, for computational efficiency, we estimate  $d(G, G')$  by truncating the FRTDs at  $t = 14$ . Starting from an initial graph  $G'$ , we propose a new graph  $G^*$  by a combination of two operations: with probability 0.4 we select an edge at random and move it, else we perform a random degree preserving rewiring. The modified graph is accepted according to the Metropolis criterion  $\min\{1, e^{-\beta(d(G^*, G) - d(G', G))}\}$ .

The inverse temperature,  $\beta$ , interpolates between uniformly random networks with the same degree sequence at  $\beta = 0$ , and graphs matching the target's FRTDs as  $\beta \rightarrow \infty$ . These distributions are difficult to sample from using MCMC [30, 39, 3], thus to traverse high-probability regions separated by large barriers of low probability we employ parallel tempering: multiple chains are run at different  $\beta$  and we periodically attempt to swap the temperatures of these chains [40, 13].

We study two examples: the Karate club network (34 nodes) [47], and the *C. elegans* connectome (297 nodes) [46, 45].

**3.3.1. Karate club.** The Monte Carlo process utilizes 50 chains with  $\beta \in [0, 70]$  initialized at a random  $G(n, m)$  graph. A burn-in period of  $2 \times 10^6$  samples is employed after which we collect samples. At large  $\beta$  the Karate club network is recovered exactly by the algorithm and as we reduce  $\beta$  we sample random graphs which resemble the original graph in several respects. In Fig. 5 we see that the samples preserve both local and global features, with the degree of preservation depending on the temperature.

As the properties of the random graphs approach the target, the entropy decreases. The entropy (which roughly measures the logarithm of the number of “typical” graphs) and the specific heat (which measures how the expected value of  $d(G', G)$  changes with  $\beta$ ) both display a change in the region  $\beta \approx 50$ , indicating phase transition like behavior. Beyond this point, a large proportion of the samples are either isomorphic to the target or differ only by very small perturbations. But, shortly before this point we see a region that still has a relatively large entropy but also preserves many properties of the graph.

**3.3.2. *C. elegans*.** For the *C. elegans* network we see a similar picture. The bottom row of Fig. 5 displays the graph statistics obtained at different  $\beta$ . As before,  $\beta$  determines the interpolation between complete randomization of the edges and FRTD preserving randomization. By increasing  $\beta$  the various graph properties are better preserved. Before a phase-transition like behavior, we see a region with non-zero entropy that still does a good job at preserving the statistics of the original graph.

To reiterate, the distribution of Eq. (3.4) is defined entirely by the FRTD. The fact that it preserves key statistics of the base graphs suggests that the FRTD itself encodes the relevant structural information.

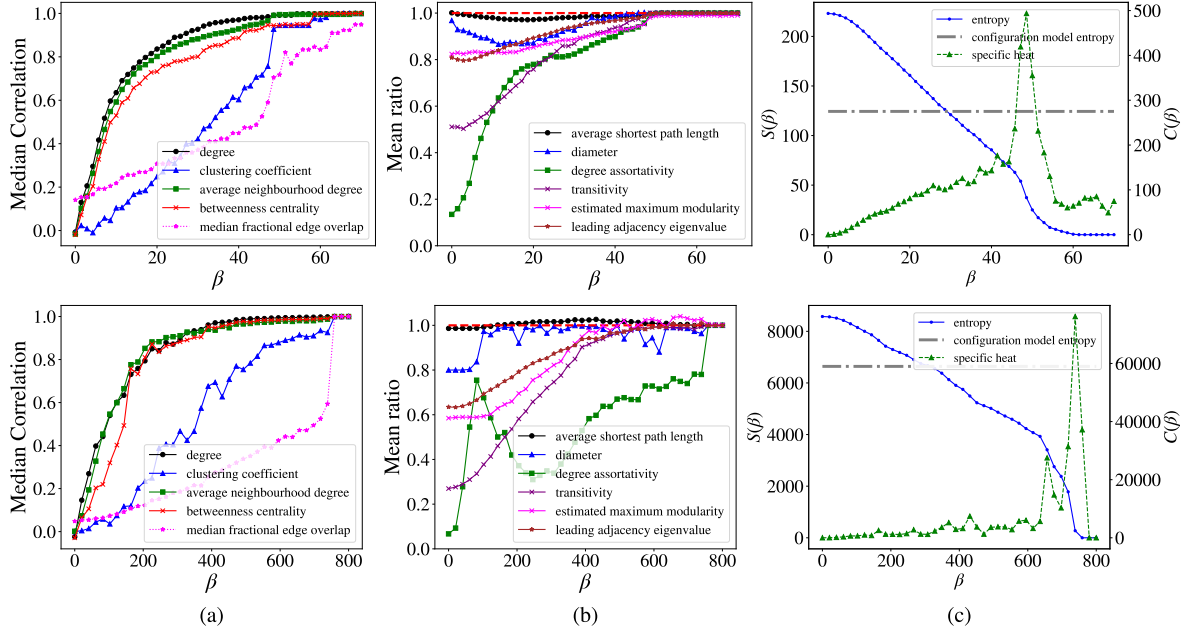


Figure 5: Graph statistics for the Karate club (top row) and *C. elegans* (bottom row). The statistics of the original network are compared with those obtained from  $P_G(G')$  at different values of  $\beta$ . At  $\beta = 0$ , we sample all graphs with the same number of edges with equal probability. Increasing  $\beta$  biases the distribution towards networks with similar FRTDs to the target. Panel (a) shows the median Pearson correlation coefficient between various node level descriptors for nodes in  $G'$  compared to  $G$ , i.e., half of the sampled graphs  $G'$  have a Pearson correlation to  $G$  which is larger than the reported median value. Panel (b) displays the average ratio of various global network descriptors for  $G'$  to  $G$ , i.e.,  $E[s(G')/s(G)]$  for graph statistic  $s$ . Panel (c) shows the entropy and specific heat of the random graph ensemble. We also show the configuration model entropy, estimated from the approximation of McKay and Wormald [26].

**4. Discussion.** In this work we have argued that the first return time distribution of a random walk captures meaningful structural information and forms an effective graph embedding method. The approach is straightforwardly extended to weighted and directed networks—see Appendix A. In addition to the theoretical results, the key evidence we provide in favor of FRTD embedding is a sequence of empirical experiments. We have demonstrated that the FRTD can be used to (i) define (and hence discover) structural roles for the nodes in a network; (ii) identify nodes across corrupted versions of the same network; and (iii) define a sensible distance between graphs which can be used to generate random graphs that are still “close” to the original.

In the role discovery experiments, the FRTD is clearly different to the more classical conception of community structure and more closely related to an intuitive notion of role or function (e.g., hub vs regional airports, main vs supporting characters).

In the alignment experiments, we find that the FRTD embedding often outperforms a hand-crafted feature vector chosen for its intuitive appeal. This suggests that a single, well-motivated feature—the FRTD—can serve as a compact and effective summary of structural information. However, as the role-extraction experiments show, the FRTD does not, in general, encode community structure. Rather than replacing community analysis, the FRTD provides complementary information.

In the randomization experiments we find that enforcing an exact match to the FRTDs can lead to a degenerate distribution, with essentially all probability mass concentrated on the original graph (consistent with the conjectures of Refs. [23, 19, 44]). However, by relaxing this constraint slightly (i.e., decreasing  $\beta$  in Eq. (3.4)), we identify a region of non-zero entropy that still approximately preserves the salient structural features.

In summary, the FRTD is an informative embedding, normalized and invariant to node relabeling, and capable of capturing structural properties in a compact form. Our results offer additional justification for the widespread use of random-walk-based statistics in machine learning, beyond the pragmatic observation that “they appear to work in practice” [48, 12]. From a practical standpoint, however, we recommend using of the FRTD rather than return probabilities.

Many open questions remain. For example, it is not yet known whether FRTDs are sufficient to uniquely identify a graph when all eigenvalues of the symmetric normalized adjacency matrix are simple. Or, on a practical level, while it is easy to compute the FRTDs from a network it is far from trivial to reverse this mapping, even approximately. The Markov chain we employ should technically achieve this for sufficiently large  $\beta$ , but the method is prohibitively slow for large networks. An efficient method to generate networks with a given random walk structure could be of great interest to both theorists and practitioners. Lastly, in this work we compute the FRTD exactly by repeated multiplication of the random walk matrix. This method however scales as  $\mathcal{O}(n^3K)$  in worst case (see Appendix A for details). To allow for greater scalability, the FRTD may also be estimated, for example by Monte Carlo [2] or message passing [22]. These algorithms would allow for efficient and decentralized embedding, but at the cost that calculations would only be approximate.

**Code and data availability.** The full code (along with publicly available links to data) to reproduce the results in this work can be found at [https://github.com/Vedanta-T/RandomWalk\\_FRTD\\_embeddings.git](https://github.com/Vedanta-T/RandomWalk_FRTD_embeddings.git).

**Acknowledgements.** We thank Erik Hormann for useful discussions. VT expresses gratitude to the Rhodes Trust and the Mathematical Institute for funding. RL acknowledges support from the EPSRC Grants EP/V013068/1, EP/V03474X/1, and EP/Y028872/1.

## REFERENCES

- [1] Y. AFLALO, A. BRONSTEIN, AND R. KIMMEL, *On convex relaxation of graph isomorphism*, Proceedings of the National Academy of Sciences, 112 (2015), pp. 2942–2947, <https://doi.org/10.1073/pnas.1401651112>.
- [2] K. AVRACHENKOV, N. LITVAK, D. NEMIROVSKY, AND N. OSIROVA, *Monte Carlo methods in PageRank computation: When one iteration is sufficient*, SIAM Journal on Numerical Analysis, 45 (2007), pp. 890–904, <https://doi.org/10.1137/050643799>.

[3] S. BHAMIDI, G. BRESLER, AND A. SLY, *Mixing time of exponential random graphs*, in 2008 49th Annual IEEE Symposium on Foundations of Computer Science, IEEE, 2008, pp. 803–812, <https://doi.org/10.1109/FOCS.2008.75>.

[4] V. D. BLONDEL, J.-L. GUILLAUME, R. LAMBIOTTE, AND E. LEFEBVRE, *Fast unfolding of communities in large networks*, Journal of Statistical Mechanics: Theory and Experiment, (2008), p. P10008, <https://doi.org/10.1088/1742-5468/2008/10/P10008>.

[5] A. BOMMAKANTI, H. R. VONTERI, K. SKITSAS, S. RANU, D. MOTTIN, AND P. KARRAS, *FUGAL: Feature-fortified unrestricted graph alignment*, in The Thirty-eighth Annual Conference on Neural Information Processing Systems, 2024, <https://doi.org/10.5220/079017-0616>.

[6] A. BROWET, *Algorithms for community and role detection in networks*, PhD thesis, Catholic University of Louvain, Louvain-la-Neuve, Belgium, 2014.

[7] H. CAI, V. W. ZHENG, AND K. C.-C. CHANG, *A comprehensive survey of graph embedding: Problems, techniques, and applications*, IEEE Transactions on Knowledge and Data Engineering, 30 (2018), pp. 1616–1637, <https://doi.org/10.1109/TKDE.2018.2807452>.

[8] T. P. CASON, *Role extraction in networks*, PhD thesis, Catholic University of Louvain, Louvain-la-Neuve, Belgium, 2012.

[9] L. DA F. COSTA, F. A. RODRIGUES, G. TRAVIESO, AND P. R. V. BOAS, *Characterization of complex networks: A survey of measurements*, Advances in Physics, 56 (2007), pp. 167–242, <https://doi.org/10.1080/00018730601170527>.

[10] C. DONNAT, M. ZITNIK, D. HALLAC, AND J. LESKOVEC, *Learning structural node embeddings via diffusion wavelets*, in Proceedings of the 24th ACM SIGKDD International Conference on Knowledge Discovery & Data Mining, Association for Computing Machinery, 2018, p. 1320–1329, <https://doi.org/10.1145/3219819.3220025>.

[11] P. DOREIAN, V. BATAGELJ, AND A. FERLIGOJ, *Generalized Blockmodeling*, Cambridge University Press, 2010, <https://doi.org/10.1017/CBO9780511584176>.

[12] V. P. DWIVEDI, A. T. LUU, T. LAURENT, Y. BENGIO, AND X. BRESSON, *Graph neural networks with learnable structural and positional representations*, in The Tenth International Conference on Learning Representations, 2022, <https://openreview.net/forum?id=wTTjnvGphYj>.

[13] D. J. EARL AND M. W. DEEM, *Parallel tempering: Theory, applications, and new perspectives*, Physical Chemistry Chemical Physics, 7 (2005), pp. 3910–3916, <https://doi.org/10.1039/B509983H>.

[14] S. FORTUNATO AND D. HRIC, *Community detection in networks: A user guide*, Physics Reports, 659 (2016), pp. 1–44, <https://doi.org/10.1016/j.physrep.2016.09.002>.

[15] F. FOUSS, M. SAERENS, AND M. SHIMBO, *Algorithms and models for network data and link analysis*, Cambridge University Press, 2016, <https://doi.org/10.1017/CBO9781316418321>.

[16] R. FRUCHT, *Graphs of degree three with a given abstract group*, Canadian Journal of Mathematics, 1 (1949), p. 365–378, <https://doi.org/10.4153/CJM-1949-033-6>.

[17] T. M. J. FRUCHTERMAN AND E. M. REINGOLD, *Graph drawing by force-directed placement*, Software: Practice and Experience, 21 (1991), pp. 1129–1164, <https://doi.org/10.1002/spe.4380211102>.

[18] A. GROVER AND J. LESKOVEC, *node2vec: Scalable feature learning for networks*, in Proceedings of the 22nd ACM SIGKDD International conference on Knowledge Discovery and Data Mining, 2016, pp. 855–864, <https://doi.org/10.1145/2939672.2939754>.

[19] W. HAEMERS, *Are almost all graphs determined by their spectrum?*, Notices of the South African Mathematical Society, 47 (2016), pp. 42–45.

[20] W. L. HAMILTON, R. YING, AND J. LESKOVEC, *Representation learning on graphs: Methods and applications*, IEEE Data Engineering Bulletin, 40 (2017), pp. 52–74, <https://api.semanticscholar.org/CorpusID:3215337>.

[21] K. HENDERSON, B. GALLAGHER, T. ELIASI-RAD, H. TONG, S. BASU, L. AKOGLU, D. KOUTRA, C. FALOUTSOS, AND L. LI, *Rolx: structural role extraction & mining in large graphs*, in Proceedings of the 18th ACM SIGKDD International Conference on Knowledge Discovery and Data Mining, 2012, pp. 1231–1239, <https://doi.org/10.1145/2339530.2339723>.

[22] E. HORMANN, R. LAMBIOTTE, AND G. T. CANTWELL, *Approximation for return time distributions of random walks on sparse networks*, Physical Review E, 111 (2025), p. 064306, <https://doi.org/10.1103/PhysRevE.111.064306>.

[23] I. KOVAL AND M. KWAN, *Exponentially many graphs are determined by their spectrum*, The Quarterly

Journal of Mathematics, 75 (2024), pp. 869–899, <https://doi.org/10.1093/qmath/haae030>.

[24] H. W. KUHN, *The hungarian method for the assignment problem*, Naval research logistics quarterly, 2 (1955), pp. 83–97, <https://doi.org/10.1002/nav.3800020109>.

[25] R. LAMBIOTTE AND M. T. SCHAUB, *Modularity and dynamics on complex networks*, Cambridge University Press, 2021, <https://doi.org/10.1017/9781108774116>.

[26] B. D. MCKAY AND N. C. WORMALD, *Asymptotic enumeration by degree sequence of graphs of high degree*, European Journal of Combinatorics, 11 (1990), pp. 565–580, [https://doi.org/10.1016/S0195-6698\(13\)80042-X](https://doi.org/10.1016/S0195-6698(13)80042-X).

[27] M. E. J. NEWMAN, *The structure and function of complex networks*, SIAM Review, 45 (2003), pp. 167–256, <https://doi.org/10.1137/S003614450342480>.

[28] M. E. J. NEWMAN, *Networks*, Oxford University Press, 2 ed., 2018, <https://doi.org/10.1093/oso/9780198805090.001.0001>.

[29] L. PAGE, S. BRIN, R. MOTWANI, AND T. WINOGRAD, *The PageRank citation ranking: Bringing order to the web.*, Technical Report 1999-66, Stanford InfoLab, November 1999.

[30] J. PARK AND M. E. J. NEWMAN, *Statistical mechanics of networks*, Physical Review E, 70 (2004), p. 066117, <https://doi.org/10.1103/PhysRevE.70.066117>.

[31] F. PEDREGOSA, G. VAROQUAUX, A. GRAMFORT, V. MICHEL, B. THIRION, O. GRISEL, M. BLONDEL, P. PRETTENHOFER, R. WEISS, V. DUBOURG, J. VANDERPLAS, A. PASSOS, D. COURNAPEAU, M. BRUCHER, M. PERROT, AND ÉDOUARD DUCHESNAY, *Scikit-learn: Machine learning in Python*, Journal of Machine Learning Research, 12 (2011), pp. 2825–2830, <http://jmlr.org/papers/v12/pedregosa11a.html>.

[32] B. PEROZZI, R. AL-RFOU, AND S. SKIENA, *Deepwalk: Online learning of social representations*, in Proceedings of the 20th ACM SIGKDD International conference on Knowledge Discovery and Data Mining, 2014, pp. 701–710, <https://doi.org/10.1145/2623330.2623732>.

[33] L. F. R. RIBEIRO, P. H. P. SAVERESE, AND D. R. FIGUEIREDO, *struc2vec: Learning node representations from structural identity*, in Proceedings of the 23rd ACM SIGKDD International Conference on Knowledge Discovery and Data Mining, 2017, pp. 385–394, <https://doi.org/10.1145/3097983.3098061>.

[34] E. S. ROBERTS AND A. C. C. COOLEN, *Unbiased degree-preserving randomization of directed binary networks*, Physical Review E, 85 (2012), p. 046103, <https://doi.org/10.1103/PhysRevE.85.046103>.

[35] R. A. ROSSI AND N. K. AHMED, *Role discovery in networks*, IEEE Transactions on Knowledge and Data Engineering, 27 (2014), pp. 1112–1131, <https://doi.org/10.1109/TKDE.2014.2349913>.

[36] R. A. ROSSI, D. JIN, S. KIM, N. K. AHMED, D. KOUTRA, AND J. B. LEE, *On proximity and structural role-based embeddings in networks: Misconceptions, techniques, and applications*, ACM Transactions on Knowledge Discovery from Data, 14 (2020), <https://doi.org/10.1145/3397191>.

[37] M. T. SCHAUB, J.-C. DELVENNE, R. LAMBIOTTE, AND M. BARAHONA, *Multiscale dynamical embeddings of complex networks*, Physical Review E, 99 (2019), p. 062308, <https://doi.org/10.1103/PhysRevE.99.062308>.

[38] K. SKITSAS, K. ORLOWSKI, J. HERMANN, D. MOTTIN, AND P. KARRAS, *Comprehensive evaluation of algorithms for unrestricted graph alignment*, in EDBT, 2023, pp. 260–272, <https://doi.org/10.48786/edbt.2023.21>.

[39] T. A. B. SNIJders, *Markov chain Monte Carlo estimation of exponential random graph models*, Journal of Social Structure, 3 (2002), pp. 1–40.

[40] R. H. SWENDSEN AND J.-S. WANG, *Replica monte carlo simulation of spin-glasses*, Physical Review Letters, 57 (1986), pp. 2607–2609, <https://doi.org/10.1103/PhysRevLett.57.2607>.

[41] R. TANG, Z. YONG, S. JIANG, X. CHEN, Y. LIU, Y.-C. ZHANG, G.-Q. SUN, AND W. WANG, *Network alignment*, Physics Reports, 1107 (2025), pp. 1–45, <https://doi.org/10.1016/j.physrep.2024.11.006>.

[42] J. T. VOGELSTEIN, J. M. CONROY, V. LYZINSKI, L. J. PODRAZIK, S. G. KRATZER, E. T. HARLEY, D. E. FISHKIND, R. J. VOGELSTEIN, AND C. E. PRIEBE, *Fast approximate quadratic programming for graph matching*, PLOS ONE, 10 (2015), pp. 1–17, <https://doi.org/10.1371/journal.pone.0121002>.

[43] U. VON LUXBURG, *A tutorial on spectral clustering*, Statistics and Computing, 17 (2007), pp. 395–416, <https://doi.org/10.1007/s11222-007-9033-z>.

[44] W. WANG AND W. WANG, *Haemers' conjecture: An algorithmic perspective*, Experimental Mathematics, 34 (2025), pp. 147–161, <https://doi.org/10.1080/10586458.2024.2337229>.

[45] D. J. WATTS AND S. H. STROGATZ, *Collective dynamics of 'small-world' networks*, Nature, 393 (1998),

pp. 440–442, <https://doi.org/10.1038/30918>.

[46] J. G. WHITE, E. SOUTHGATE, J. N. THOMSON, AND S. BRENNER, *The structure of the nervous system of the nematode Caenorhabditis elegans: the mind of a worm*, Philosophical Transactions of the Royal Society B, 314 (1986), pp. 1–340, <https://doi.org/10.1098/rstb.1986.0056>.

[47] W. W. ZACHARY, *An information flow model for conflict and fission in small groups*, Journal of Anthropological Research, 33 (1977), pp. 452–473, <http://www.jstor.org/stable/3629752>.

[48] Z. ZHANG, M. WANG, Y. XIANG, Y. HUANG, AND A. NEHORAI, *RetGK: Graph kernels based on return probabilities of random walks*, in Proceedings of the 32nd International Conference on Neural Information Processing Systems, vol. 31, 2018, [https://proceedings.neurips.cc/paper\\_files/paper/2018/file/7f16109f1619fd7a733daf5a84c708c1-Paper.pdf](https://proceedings.neurips.cc/paper_files/paper/2018/file/7f16109f1619fd7a733daf5a84c708c1-Paper.pdf).

**Appendix A. Computing FRTDs.** The distribution  $f_i(t)$  can be computed for all  $i$  by matrix multiplication. The following algorithm achieves this.

---

**Algorithm A.1** Algorithm to compute FRTDs

**Input:**  $(n \times n)$  transition matrix  $\mathbf{T} = \mathbf{D}^{-1}\mathbf{A}$  and maximum number of steps,  $K$ .

```

1:  $\mathbf{P} \leftarrow \text{Identity}(n)$ 
2:  $\mathbf{f} \leftarrow \text{zeros}((n, K + 1))$ 
3: for  $t$  in  $1 : K$  do
4:    $\mathbf{P} \leftarrow \mathbf{T}\mathbf{P}$ 
5:    $\mathbf{f}[:, t] \leftarrow \text{diagonal}(\mathbf{P})$ 
6:    $\text{diagonal}(\mathbf{P}) = \mathbf{0}$ 
7: end for
8:  $\mathbf{f}[:, K + 1] \leftarrow \mathbf{1} - \mathbf{f} \mathbf{1}$ 
9: return  $\mathbf{f}$ 
```

---

When  $\mathbf{A}$  is sparse then the matrix multiplication  $\mathbf{T}\mathbf{P}$  requires  $\mathcal{O}(n^2)$  operations and hence the full algorithm runs in  $\mathcal{O}(Kn^2)$ . If  $\mathbf{A}$  is not sparse, it will take  $\mathcal{O}(Kn^3)$  operations. Note, in order to produce a normalized embedding the remaining probability mass is appended, i.e.,  $f[i, K + 1] \leftarrow 1 - \sum_{t=1}^K f[i, t]$ .

**A.1. FRTDs for directed networks.** The above definitions can be extended to construct FRTDs for directed networks by introducing “teleportation” to avoid getting stuck at sets of nodes with no outward edges. At each step the random walker will move by an outgoing edge with probability  $1 - \alpha$  or alternatively with probability  $\alpha$  it will “teleport” by jumping to any node in the network with equal probability. The transition matrix is thus

$$(A.1) \quad (1 - \alpha)\mathbf{D}^{-1}\mathbf{A} + (\alpha/n)\mathbf{1}$$

where  $\mathbf{1}$  is a matrix of all ones. Typically  $\alpha$  is chosen to be  $\alpha = 0.15$ , as originally suggested in the PageRank algorithm [29].

For an informative embedding that depends on both in-edges and out-edges, we use the FRTD of the transition matrix of Eq. (A.1), together with the same distribution but on the reversed graph, i.e. with  $\mathbf{A}$  replaced by  $\mathbf{A}^T$ .

**A.2. Example.** As an illustration of the above we study randomization of the directed *C. elegans* graph (in the sense of Sec. 3.3). To improve the mixing time we fix the degree

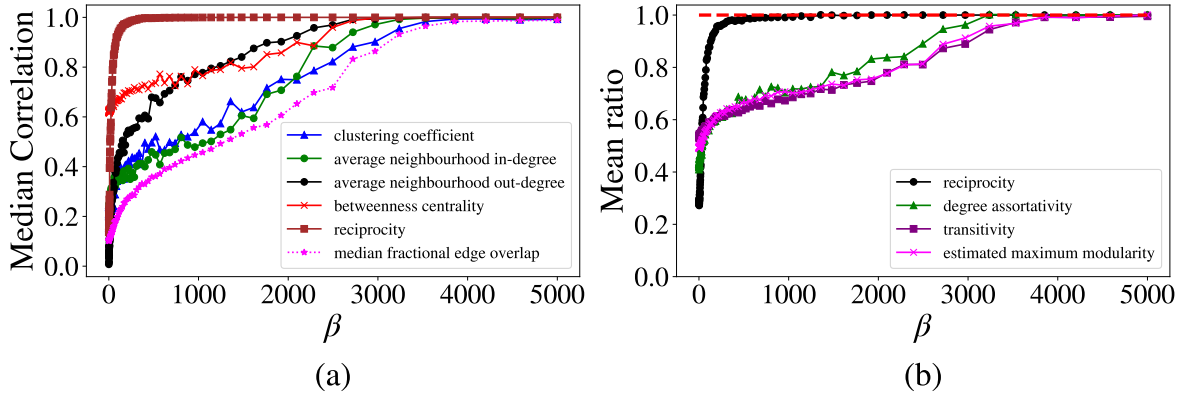


Figure 6: Graph statistics for the directed *C. elegans* connectome compared with those obtained from  $P_G(G')$  at different temperatures, note that  $\beta = 0$  corresponds to sampling all graphs with the same in- and out-degree sequence with equal probability. Panel (a) shows the median correlation between various node level descriptors of samples  $G'$  and  $G$ , (b) displays the ratio of various global network descriptors for  $G'$  vs  $G$ .

cluster	airport size		
	small	medium	large
1	259	509	26
2	136	1456	29
3	2	237	387

Table 1: Relationship between the FRTD clusters and the small/medium/large designation of the airports.

sequence of the random graphs and candidates are proposed only using the degree preserving rewiring method described in [34]. One hundred chains with  $\beta \in [0, 5000]$  are initialized at  $G$  and a burn-in period of  $2 \times 10^5$  steps is used before collecting samples. Fig. 6 shows the statistics of the samples. This directed version of the model interpolates between the directed configuration model at  $\beta = 0$  and a model that preserves the full FRTD for both  $\mathbf{A}$  and  $\mathbf{A}^T$  as  $\beta \rightarrow \infty$ .

**Appendix B. Spectral clustering and metadata.** In Table 1 we report how the three clusters found by the FRTD in the airports network relate to the small/medium/large airport designations.

In Table 2, we report the names of the characters in the Lord of the Rings network, and state which FRTD cluster they were placed in.

**Appendix C. Index of datasets for graph alignment.** We follow Ref. [38], which reviews graph alignment methods using a standard dataset of 18 networks of varying sizes and domains. Table 3 provides their details along with an index corresponding to the  $x$  axis labels in Fig. 4.

cluster	characters
1	Aragorn, Frodo, Bilbo, Boromir, Merry, Denethor, Elrond, Eomer, Faramir, Galadriel, Sam, Gandalf, Gimli, Gollum, Legolas, Saruman, Theoden, Pippin, Wormtongue, Sauron
2	Arod, Arwen, Beorn, Beregond, Bergil, Fredegar Bolger, Tom Bombadil, Celeborn, Derufin, Duilin, Dain, Elladan and Elrohir, Eowyn, Erestor, Bill Ferny, Forlong, Glorfindel, Gorbag, Grimbald, Gwaihir, Halbarad, Haldir, Harding, Hasufel, Herefara, Herubrand, Hirluin, Hurin, Hama, Imrahil, Ingold, Ioreth, Mablung, Maggot, Nob, Radagast, Rumil, Ted Sandyman, Shagrat, Shelob, Thranduil, Theodred, Treebeard, Ugluk, Will Whitfoot, Windfola, Angmar
3	Anborn, Asfaloth, Willie Banks, Baranor, Beechbone, Bob, Folco Boffin, Melilot Brandybuck, Bregalad, Barliman Butterbur, Ceorl, Rosie Cotton, Cirdan, Damrod, Dervorin, Duinhir, Durin's Bane, Dunhere, Elfhelm, Erkenbrand, Fastred, Fimbrethil, Finglas, Firefoot, Fladrif, Galdor, Gamling, Ghan-buri-Ghan, Gildor Inglorion, Golasgil, Goldberry, Gothmog, Grimbeorn, Grishnakh, Mat Heathertoes, Hob Hayward, Lagduf, Landroval, Lindir, Lugdush, Mauhur, Meneldor, Mouth of Sauron, Muzgash, Willow, Noakes, Orophin, Odo Proudfoot, Sancho Proudfoot, Radbug, Robin Smallburrow, Snaga, Targon, The King of the Dead, Everard Took, Daddy Twofoot, Ufthak, Watcher in the Water, Widow Rumble, Widfara

Table 2: Character assignment to FRTD clusters in the Lord of the Rings network.

datasets					results [accuracy] [time(s)]		
index	name	n	m	type	FRT	FUGAL	FUGAL-FRT
0	ca-netscience	379	914	Collaboration	0.550 ± 0.007	0.668 ± 0.000	0.661 ± 0.007
					0.108 ± 0.002	3.079 ± 0.036	2.222 ± 0.058
1	inf-euroroad	1174	1417	Infrastructure	0.502 ± 0.011	0.747 ± 0.020	0.528 ± 0.008
					1.137 ± 0.412	14.123 ± 0.830	9.858 ± 0.006
2	bio-celegans	453	2025	Biological	0.562 ± 0.012	0.538 ± 0.023	0.817 ± 0.022
					1.301 ± 0.018	4.256 ± 0.028	4.152 ± 0.013
3	in-arenas	1133	5399	Infrastructure	0.648 ± 0.011	0.807 ± 0.045	0.884 ± 0.010
					1.885 ± 0.133	18.273 ± 0.050	18.688 ± 0.054
4	inf-power	4941	6594	Infrastructure	0.506 ± 0.010	0.630 ± 0.016	0.505 ± 0.010
					31.538 ± 1.721	1013.999 ± 11.035	461.960 ± 1.399
5	ca-Erdos992	5094	7515	Collaboration	0.222 ± 0.003	0.292 ± 0.003	0.249 ± 0.003
					32.595 ± 1.145	1122.475 ± 1.156	498.791 ± 0.787
6	ca-GrQc	4158	13422	Collaboration	0.510 ± 0.008	0.287 ± 0.007	0.554 ± 0.013
					25.477 ± 0.039	700.845 ± 0.006	717.982 ± 0.765
7	soc-hamsterster	2426	16630	Social	0.448 ± 0.008	0.366 ± 0.003	0.595 ± 0.005
					12.621 ± 0.051	185.681 ± 0.608	196.021 ± 0.155
8	bio-dmela	7393	25569	Biological	0.437 ± 0.001	0.262 ± 0.053	0.584 ± 0.001
					94.028 ± 7.124	3157.374 ± 6.624	2642.664 ± 1.773
9	socfb-Haverford76	1446	59589	Social	0.390 ± 0.004	0.340 ± 0.006	0.768 ± 0.016
					18.178 ± 0.381	42.819 ± 0.007	49.867 ± 0.107
10	socfb-Swarthmore42	1659	61050	Social	0.392 ± 0.012	0.646 ± 0.111	0.954 ± 0.030
					25.413 ± 0.241	80.465 ± 0.097	96.319 ± 0.414
11	socfb-Bowdoin47	2252	84387	Social	0.429 ± 0.0021	0.175 ± 0.033	0.823 ± 0.026
					48.168 ± 0.786	168.275 ± 0.248	202.938 ± 0.197
12	soc-facebook	4039	87352	Social	0.553 ± 0.016	0.158 ± 0.004	0.739 ± 0.003
					95.339 ± 1.186	658.184 ± 1.422	732.166 ± 4.983
13	socfb-Hamilton46	2314	96394	Social	0.415 ± 0.001	0.134 ± 0.007	0.872 ± 0.002
					57.185 ± 0.321	181.555 ± 0.220	222.257 ± 0.380
14	CA-AstroPh	17903	195004	Collaboration	0.449 ± 0.002	0.082 ± 0.000	0.577 ± 0.001
					1207.700 ± 2.354	41798.393 ± 1268.389	44002.664 ± 169.846
15	Voles*	713	2322	Proximity	0.742	0.978	0.983
					0.521	6.342	6.052
16	HighSchool*	327	5818	Proximity	0.281	0.960	1.000
					0.423	3.694	2.985
17	MultiMagna*	1004	8323	Biological	0.655	0.361	0.33
					1.797	13.334	13.756

Table 3: List of datasets and accuracy results used for numerical experiments on graph alignment using FRTDs and the existing FUGAL [5] algorithm previously used for a review in Ref. [38]. The indices correspond to the labels in Fig. 4. The datasets marked with an asterisk refer to ‘real noise’ networks—networks where multiple noisy copies are available and these are aligned to each other rather than to copies with artificial noise. *Voles* and *HighSchool* are temporal proximity networks, where the final network is aligned to a previous variant containing 95% of edges. *MultiMagna* is a protein-protein interaction network for yeast, in this case the ‘best’ network is aligned to a noisy variant containing an additional 5% of low confidence interactions.